© 2025 IEEE. Personal use of this material is permitted. Permission from IEEE must be obtained for all other uses, in any current or future media, including reprinting / republishing this material for advertising or promotional purposes, creating new collective works, for resale or redistribution to server or lists, or reuse of any copyrighted component of this work in other works.

Joint Training of Predistortion, Power Back-Off and Constellation for Satellite Power Amplifiers using Neural Networks

David Kopyto, Marius Tietze and Gerhard Bauch
Institute of Communications
Hamburg University of Technology
Hamburg, Germany
{david.kopyto, marius.tietze, bauch}@tuhh.de

***Abstract*—The deployment of satellite mega constellations may enable global coverage, even for direct transmission from satellite to handheld device. Such transmissions come with increased demands in power efficiency. The traveling wave-tube amplifier (TWTA) in satellite payloads fundamentally limits the transmit power and causes distortions to the transmit signal when power efficient transmission close to amplifier saturation is desired. This work introduces a novel joint training paradigm of constellation, amplifier power back-off and data predistortion to maximize the throughput of single carrier transmission over transparent satellite links. The joint design is enabled by means of communication autoencoders, where transmitter and receiver components are adapted together to achieve the lowest bit error rate (BER). We show how constrained constellation optimization can improve performance on selected configurations from the broadcasting standard DVB-S2X. Results are presented in terms of coded BER and information rates.**

***Index Terms*—digital predistortion, satellite communications, constellation shaping, autoencoders**

I. Introduction

Future satellite mega constellations require the manufacturing of an increased number of satellites. The maximization of throughput for transmission over the satellite payload is therefore a crucial research question to reduce hardware cost in satellite mega constellations [1]. The throughput can be maximized by designing transmit signals, which operate close to amplifier saturation with high efficiency [2], [3]. Motivated by the need for such efficient signals, this work provides a novel neural network-based communication chain to maximize the throughput on satellite payloads with power amplifier nonlinearity.

Satellite payloads are usually equipped with a traveling wave-tube amplifier (TWTA) to amplify the signal for robust transmission from orbit to earth. To maximize the energy efficiency, the transmit signal may be optimized for transmission close to TWTA saturation.

In such conditions, the amplifier operates highly nonlinear, resulting in in-band and out-of-band distortions. In satellite communications, particularly in-band distortions need to be mitigated, as out-of-band distortions are typically limited by an analog output multiplexer (OMUX) filter at the amplifier output.

We develop our system based on the satellite broadcasting standard DVB-S2X [4], as this standard provides detailed insights into satellite channel conditions and defines dedicated transmission schemes. More specifically, DVB-S2X defines optimized transmit signals for different amplifier operation points and signal-to-noise ratios (SNRs). The definition includes optimized amplitude and phase-shift keying (APSK) constellations with their recommended amplifier input back-off (IBO) for various modulation orders and code rates. These so-called modulation and coding schemes (MODCODs) offer highly reliable performance with reduced in-band distortions for dedicated channel conditions.

Additionally, data predistortion can be applied at the transmitter, which further reduces the impairments [2], [5]. Traditionally, the optimization of constellation, power back-off and data predistortion is done separately. The optimization of the DVB-S2X constellations was done for the additive white Gaussian noise (AWGN) channel, which is detailed in [6]. To find the optimal power back-off, total degradation analysis is typically carried out [7] for a specific constellation. For the found back-off and constellation, the amplifier distortions are minimized by predistortion [5]. Even though DVB-S2X details this sequential approach, the DVB-S2X documentation [4] states, that for nonlinear channels may be jointly optimized with nonlinear predistortion devices in the uplink station for the selected operating point of the nonlinear channel amplifier.

To the best of our knowledge, such a joint optimization of constellation, power back-off and predistortion has not been proposed to date. Hence, this paper proposes a joint approach by leveraging communication autoencoders [8], [9]. Based on our previous work, where we optimized IBO and constellation on a discrete TWTA channel [10], and our recently proposed recurrent neural network (RNN) data predistortion [5], we now combine these two findings to propose an RNN autoencoder for transparent satellite payloads.

In this work, we show, how neural network training can maximize the mutual information for satellite links by finding the best IBO, constellation and predistortion. We present optimized constellations with their corresponding IBO and data predistortion and argue, that by the flexibility of au-

toencoder training, DVB-S2X baseline constellations can be outperformed. We present our results by means of bit error rate (BER) and achievable information rate (AIR) analysis using the DVB-S2X low density parity check (LDPC) code.

II. System Model

We consider a single carrier baseband model of transmission over a transparent satellite payload, as depicted in Fig. 1. A neural transceiver with weights $\boldsymbol{\theta}_{\text{TX}}$ transmits symbols $\mathbf{c}_{\text{IN}}$ from a bitstream $\mathbf{b}$ via a pulse shaping filter $g(t)$ with roll-off factor α to the transparent satellite. The payload consists of an input multiplexer (IMUX) filter, TWTA and an OMUX filter. The signal is corrupted by AWGN downlink noise $n(t)$ and a receive filter, which is matched to the pulse shaping filter, i.e., $g^*(-t)$ is applied. A neural demapper with weights $\boldsymbol{\theta}_{\text{RX}}$ estimates soft bits $\hat{\mathbf{b}}$ from the received symbols $\mathbf{y}$.

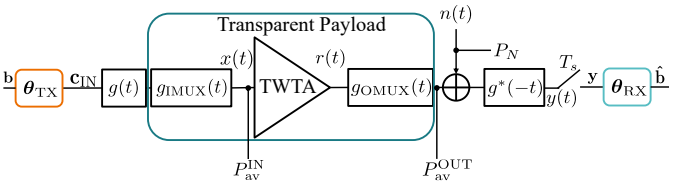

Fig. 1: Channel model with pulse shaping, transparent payload, noise and matched filter.

A. Transparent Payload

Transparent satellite payloads amplify the signal transmitted from the ground station and forward it to the receiver earth station. To do so, the payload is equipped with three main analog components, as displayed in the channel model in Fig. 1. First, an IMUX filter with impulse response $g_{\text{IMUX}}(t)$ filters out adjacent signals close to the useful band. The TWTA amplifies the analog signal to ensure robust transmission to the ground station. To cut out out-of-band radiations caused by nonlinear operation of the TWTA, the OMUX filter with response $g_{\text{OMUX}}(t)$ is used. The responses of IMUX and OMUX filters are detailed in [11].

For the amplifier, we consider a memoryless nonlinearity with amplitude and phase variations in response to amplitude variations of an input signal $x(t)$:

$$r(t) = v(|x(t)|)e^{j[\phi(t)+\vartheta(|x(t)|)]} \tag{1}$$

where $\phi(t)$ is the initial phase of the input signal.

The TWTA is modeled by the so-called memoryless Saleh model [12]. The Saleh model defines the nonlinear amplitude conversion $v(a)$ and the nonlinear phase conversion $\vartheta(a)$ as:

$$v(a) = \frac{\alpha_v a}{\beta_v a^2 + 1}, \tag{2}$$

$$\vartheta(a) = \frac{\alpha_\vartheta a^2}{\beta_\vartheta a^2 + 1}. \tag{3}$$

As $v(a)$ has a global maximum, i.e., a saturation point, the TWTA is, hence, limited by a maximum input $P_{\text{sat}}^{\text{IN}}$ and output power $P_{\text{sat}}^{\text{OUT}}$. As coefficients, we choose $\alpha_v = 2$, $\beta_v = 1$, $\alpha_\vartheta = \pi/3$ and $\beta_\vartheta = 2$ within this work, which ensures $P_{\text{sat}}^{\text{OUT}} = 1$ [5].

B. Signal-to-Noise Ratio

At the output of the satellite payload, downlink AWGN with noise power $P_N = \sigma_N^2$ is added to the signal. As the payload output is power-limited by $P_{\text{sat}}^{\text{OUT}}$, the effective SNR is not only determined by the noise power P_N, but by the operation point of the power amplifier. To this end, we define the operation point via the power back-off at amplifier input (IBO) and output (output back-off (OBO)):

$$\text{IBO} = \frac{P_{\text{sat}}^{\text{IN}}}{P_{\text{av}}^{\text{IN}}}, \tag{4}$$

$$\text{OBO} = \frac{P_{\text{sat}}^{\text{OUT}}}{P_{\text{av}}^{\text{OUT}}}. \tag{5}$$

Within this work, we design the transmit signal by variation of transmit constellation, predistortion and IBO. The variation of these components will cause a change of the average amplifier input power $P_{\text{av}}^{\text{IN}}$ and hence the average power at the amplifier output $P_{\text{av}}^{\text{OUT}}$, which is the effective transmit power of the downlink signal. The effective SNR of the transmission is, hence, defined as:

$$\text{SNR}_{\text{eff}} = \frac{P_{\text{av}}^{\text{OUT}}}{P_N}. \tag{6}$$

As we train the transmitter to optimize the operation point of the amplifier, the average power at input and output is, however, not constant. This makes effective SNR incompatible for performance analysis of AWGN channels with peak power constraints.

A more appropriate SNR measure is the peak signal-to-noise ratio (PSNR), which is defined via the maximum amplifier output power:

$$\text{PSNR} = \frac{P_{\text{sat}}^{\text{OUT}}}{P_N}. \tag{7}$$

In contrast to the average power, the output power at saturation $P_{\text{sat}}^{\text{OUT}}$ is defined by the amplifier input-output characteristic and, hence, constant.

C. Channel Model

Maximizing the throughput in a communication channel usually means to maximize the SNR. As the transmit power in a power amplifier is limited by $P_{\text{sat}}^{\text{OUT}}$, maximizing the SNR means to let $\text{SNR}_{\text{eff}} \to \text{PSNR}$. However, the nonlinear power amplifier (1) causes nonlinear distortions, which appear as intersymbol interference (ISI) and warping effects and increase when $\text{SNR}_{\text{eff}} \to \text{PSNR}$. To derive this effect, we write the memoryless model (1) as a power series, i.e.,

$$v(|x(t)|)e^{j[\phi(t)+\vartheta(|x(t)|)]} = x(t)\sum_{\ell=1}^{\infty}\gamma_\ell |x(t)|^{\ell-1}. \tag{8}$$

The input signal to the power amplifier $x(t)$ is composed by the data symbols c_k, the pulse shaping filter $g(t)$ and the IMUX filter $g_{\text{IMUX}}(t)$. For brevity, let $\tilde{g}(t) := g_{\text{IMUX}}(t) * g(t)$ and $\bar{g}(t) := g^*(-t) * g_{\text{OMUX}}(t)$. Then, the input signal reads:

$$x(t) = \sum_{k=0}^{N-1} c_k \tilde{g}(t - kT_s). \tag{9}$$

With that, we write the TWTA output:

$$r(t) = x(t)\sum_{\ell=1}^{\infty}\gamma_\ell |x(t)|^{\ell-1} = \sum_{k=0}^{N-1} c_k\tilde{g}(t-kT_s)\sum_{\ell=1}^{\infty}\gamma_\ell\left|\sum_{k=0}^{N-1} c_k\tilde{g}(t-kT_s)\right|^{\ell-1}. \quad (10)$$

With the OMUX filter and matched filter, the signal at the receiver $y(t)$ will be:

$$y(t) = \bar{g}(t) * r(t) + g^*(-t) * n(t). \quad (11)$$

We can group the output signal $y(t)$ into linear and nonlinear distortions by isolating the linear term $l = 1$ in (10) and taking $\bar{g}(t)$ into account:

$$y(t) = \underbrace{\bar{g}(t) * \left[\gamma_1 \sum_{k=0}^{N-1} c_k\tilde{g}(t-kT_s)\right]}_{\text{linear signal}} + g^*(-t) * n(t) + \underbrace{\bar{g}(t) * \left[\sum_{k=0}^{N-1} c_k\tilde{g}(t-kT_s)\sum_{\ell=2}^{\infty}\gamma_\ell\left|\sum_{k=0}^{N-1} c_k\tilde{g}(t-kT_s)\right|^{\ell-1}\right]}_{\text{nonlinear distortion } d_{\text{NLIN}}}. \quad (12)$$

Please note, that in many practical systems, the receiver filter is only matched to the pulse shaping filter $g(t)$. This means, that IMUX and OMUX filter may cause additional linear distortions d_{LIN} at the matched filter output. The output symbols are therefore distorted by AWGN and ISI:

$$y_k = y(t)|_{t=kT_s} = \gamma_1 c_k + n'_k + d_{\text{LIN}} + d_{\text{NLIN}}, \quad (13)$$

with noise $n'_k = \int_{-\infty}^{\infty} n(t)g^*(-t+\tau)d\tau|_{t=kT_s}$. The nonlinear distortion d_{NLIN} consists of ISI and warping, which can be derived by using Volterra theory [13]. We leave this derivation for the Saleh model up to further research. For cubic nonlinearities, warping and ISI have been quantified this way in [14].

The result in (12) shows, that nonlinear distortions increase, when the power amplifier is driven close to its saturation point. If the input signal operates close to the saturation point of the amplifier, the values of the higher order coefficients γ_ℓ increase in the power series (12), as in this case, the slope of (2) deviates from a linear function (compression). Hence, the nonlinear distortion d_{NLIN} will increase. The increase of d_{NLIN} induces a trade-off between nonlinear distortions and average output power $P_{\text{av}}^{\text{OUT}}$. By increasing SNR_{eff}, d_{NLIN} is increased as well. We can, however, optimize transmit symbols c_k, IBO and leverage predistortion to minimize d_{NLIN}. For a constant PSNR, the best trade-off between d_{NLIN} and $P_{\text{av}}^{\text{OUT}}$ can be found.

D. Communication Autoencoder

As illustrated in Fig. 1, the processing chain consisting of transmitter, channel with payload and receiver is implemented as a communication autoencoder [8]. An autoencoder consists of an encoder neural network, here the transmitter, with weights $\boldsymbol{\theta}_{\text{TX}}$ (see Fig. 2), a latent space (the channel) and a decoder neural network, here the receiver, with weights $\boldsymbol{\theta}_{\text{RX}}$ (see Fig. 4). As explained in [9], [15], the binary cross-entropy (BCE) loss can be used to train the weights of transmitter and receiver jointly to maximize the bit-wise mutual information of the transmission and, hence, the throughput.

Let N be the block size of the l-th bit vector $\mathbf{b}_{(l)} \in \{0,1\}^{\text{N}}$ in a batch of size B. Furthermore, let $\hat{\mathbf{b}}_{(l)} \in [0,1]^{\text{N}}$ denote the l-th soft bit vector in the batch estimated by the receiver. The BCE loss between $\mathbf{b}_{(l)}$ and $\hat{\mathbf{b}}_{(l)}$ is then defined by $\text{BCE}(\mathbf{b}_{(l)}, \hat{\mathbf{b}}_{(l)}) =$

$$\frac{1}{\text{N}}[-\mathbf{b}_{(l)}^T \cdot \log_2 \hat{\mathbf{b}}_{(l)} - (\mathbf{1} - \mathbf{b}_{(l)}^T) \cdot \log_2(\mathbf{1} - \hat{\mathbf{b}}_{(l)})]. \quad (14)$$

By sending batches of bit vectors through the autoencoder, the transmitter and receiver weights $\boldsymbol{\theta}_{\text{TX}}, \boldsymbol{\theta}_{\text{RX}}$ can be trained by minimizing

$$\mathcal{L}(\boldsymbol{\theta}_{\text{TX}}, \boldsymbol{\theta}_{\text{RX}}) \approx \frac{1}{B}\sum_{l=1}^{B} \text{BCE}(\mathbf{b}_{(l)}, \hat{\mathbf{b}}_{(l)}). \quad (15)$$

Transmitter Model: The goal of this work is to design the transmit signal to find the best trade-off between average amplifier output power $P_{\text{av}}^{\text{OUT}}$ and distortions $d_{\text{LIN}} + d_{\text{NLIN}}$. We propose to design the transmit signal by a neural network, which only manipulates the signal at symbol level. The transmitter architecture is depicted in Fig. 2. The neural network consists of a neural mapper, which optimizes the constellation $\mathcal{C}$ jointly with data predistortion [5]. The data predistortion is implemented by a bidirectional RNN, which learns the ISI produced by the satellite payload. By leveraging the residual connection from mapper to RNN output, we ensure, that an inverse ISI $\mathbf{c}_{\text{RES}}$ is added to the nominal constellation symbols $\mathbf{c}_{\text{static}} \in \mathcal{C}$, resulting in a slightly modified effective transmit symbol $\mathbf{c}_{\text{DPD}}$. The scaling block learns the IBO of the transmit signal, as discussed in [10]. Hence, it adjusts the $P_{\text{av}}^{\text{IN}}$ to achieve the best trade-off between average amplifier output power $P_{\text{av}}^{\text{OUT}}$ and nonlinear distortions d_{NLIN}.

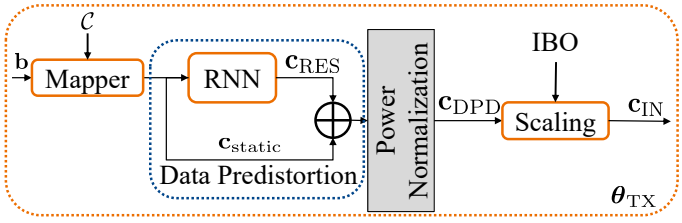

Fig. 2: Transmitter model with weights $\boldsymbol{\theta}_{\text{TX}}$. The constellation $\mathcal{C}$ and the IBO are trainable parameters, while data predistortion is realized by an RNN with residual connection.

For constellation optimization, we use different constrained optimization techniques. First, quadrant-symmetric optimization of the constellation is analyzed. Here, only the first quadrant $\mathcal{C}_I$ of the constellation is trained, and mapped to the other three quadrants to ensure constellation symmetry. Quadrant symmetry is illustrated in Fig. 3a. This method

reduces the number of trainable parameters to $M/2$, where M is the constellation size of the complex constellation, which in total has $2M$ parameters, inphase and quadrature components. Such constellations are known as non-uniform constellation (NUC) and have been introduced in the standard ATSC 3.0 [16].

As an alternative, we propose to train APSK constellations in two ways. First, only the phases and radii of each ring in a regular APSK constellation are trained. This shaping technique corresponds to static predistortion and has been used in [5]. As another approach, we propose to train the radii of the rings, while allowing arbitrary phase shifts of all points on each ring. This optimization technique is illustrated in Fig. 3b. Training APSK constellations is motivated by their usage in DVB-S2X due to their excellent performance on the AWGN channel while maintaining lowered peak-to-average power ratio (PAPR) compared to quadrature amplitude modulation (QAM).

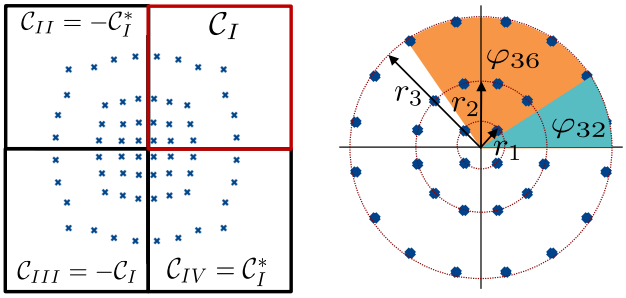

(a) NUC optimization. (b) APSK optimization.

Fig. 3: Illustration of constrained constellation shaping. In NUC optimization, only the constellation points in the first quadrant $\mathcal{C}_I$ are trained and then reflected at the axes. In APSK optimization, a regular APSK is used initially, where all radii (r_1, r_2, r_3 in the example) are optimized together with the phases of all constellation points (the phases φ_{32} and φ_{36} of the third ring and second and sixth point are highlighted as examples).

Receiver Model: The receiver is implemented as a feed-forward neural network, as depicted in Fig. 4. By doing so, we ensure, that at the receiver, only decision regions for detection of the transmit symbols are learned and soft bits $\hat{\mathbf{b}}$ are computed from the decision regions, which are used for evaluating the BCE loss function (15). Using a neural network for detection has been shown to be superior to a Gaussian detector [5], as the output symbols deviate from a purely Gaussian distribution, as explained in [17]. Hence, ISI compensation is done exclusively at the transmitter, and the neural demapper treats the remaining interference as additional noise and finds the best decision regions for the joint channel (13).

III. Results

A. Simulation Setup

Within our simulations, we illustrate how the proposed autoencoder offers a flexible and competitive alternative to

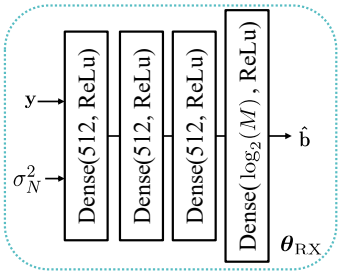

Fig. 4: Receiver model with weights $\boldsymbol{\theta}_{\mathrm{RX}}$. The receiver is implemented by three dense layers to train a memoryless neural demapper, which produces soft bits $\hat{\mathbf{b}}$ from received symbols $\mathbf{y}$ and noise variance σ_N^2.

the sequential optimization from DVB-S2X. We provide information rates and BER results on specific MODCODs of DVB-S2X. A MODCOD defines optimized APSK constellations for different modulation orders M and dedicated code rates R. The implementation guidelines of DVB-S2X [11] state optimized IBO values and PSNR for quasi error-free transmission on an idealized hard limiter channel with roll-off factor $\alpha = 0.1$ of the pulse shaping filter $g(t)$.

In this section, the performance of different autoencoder trainings on selected code rates and modulation orders is detailed. In particular, we compare NUC constellations and shaped APSK constellations to the DVB-S2X APSK in MODCODs 20/30 ($M = 256$) and 4/5 ($M = 64$). For the DVB-S2X constellations we train the autoencoder in two ways: first, only the data predistortion is learned while keeping the constellation fixed and using the IBO values recommended in [11]. This setting corresponds to [5]. Second, we fix the constellation but train the IBO together with predistortion.

For training, we use a batch size of $B = 1024$ with 5000 iterations for $M = 64$ and 20000 iterations for $M = 256$ in the first training phase. The roll-off factor $\alpha = 0.1$ has been chosen as recommended in [11]. To reach excellent performance for all autoencoders, we train them such that the BER is minimized for the specific R of the considered MODCOD. Hence, we train the models in a PSNR range close to the recommended PSNR from [11] for each MODCOD. The recommended PSNR for $R = 4/5$ and $M = 64$ is PSNR $= 19.54\,\mathrm{dB}$. To achieve robustness, we first train the autoencoder around this PSNR, i.e., for $R = 4/5$ and $M = 64$ in the interval PSNR $\in [19.0, 20.3]\,\mathrm{dB}$. In the second training phase, we fine-tune the models on the exact recommended PSNR $= 19.54\,\mathrm{dB}$ for 1000 iterations. We experienced a significant improvement in performance with this second fine-tuning phase. For $R = 20/30$ and $M = 256$ the recommended PSNR $= 21.89\,\mathrm{dB}$. We trained these models on PSNR $\in [21.0, 21.89]\,\mathrm{dB}$ in the first phase and fine-tuned on PSNR $= 21.75\,\mathrm{dB}$ for 1000 iterations. The simulation setup was built on top of the open source library Sionna [18]. The simulation parameters are summarized in Table I.

The BER results are based on coded transmission with the DVB-S2X LDPC code with the considered code rates and

MODCOD	B	Iter. Phase 1	Iter. Fine-Tuning	PSNR Phase 1	PSNR Fine-Tuning	PSNR quasi error-free [11]	IBO from [11]
$R = 4/5$ and $M = 64$	1024	5000	1000	$[19.0, 20.3]$ dB	PSNR $= 19.54$ dB	19.54 dB	3.25 dB
$R = 20/30$ and $M = 256$	1024	20000	1000	$[21.0, 21.89]$ dB	PSNR $= 21.75$ dB	21.89 dB	4.25 dB

TABLE I: Training parameters.

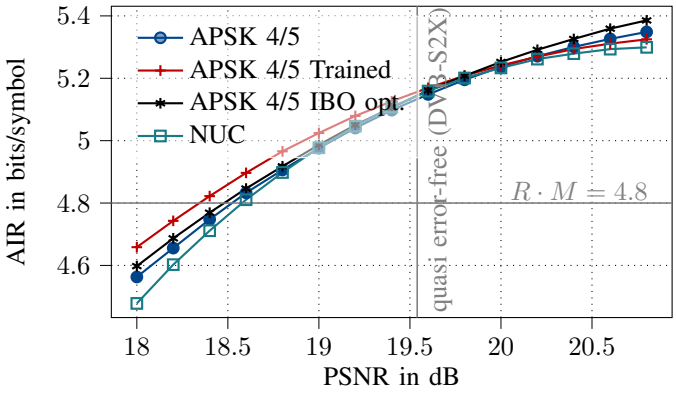

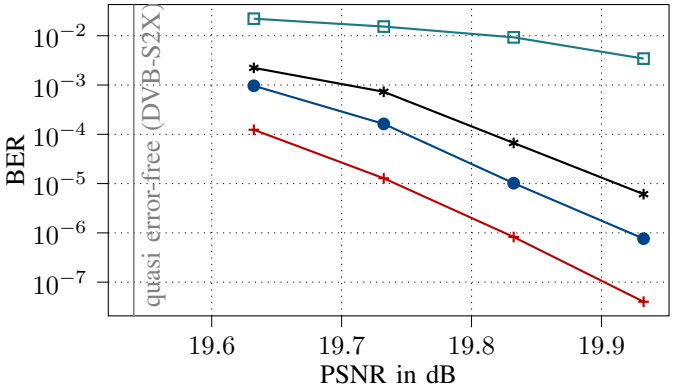

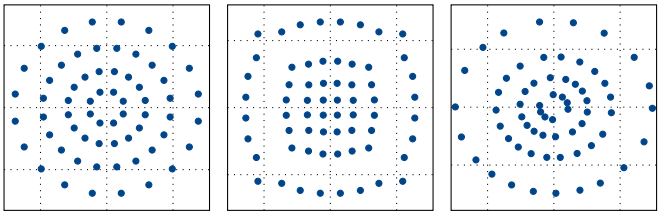

(a) APSK MODCOD 4/5 DVB-S2X.

(b) NUC.

(c) APSK trained based on MODCOD 4/5.

Fig. 5: AIR, BER and trained constellations for $R = 4/5$ and $M = 64$.

frame length N $= 64800$.

B. Bit Error Rates and Information Rates

MODCOD 4/5 Modulation Order 64: In Fig. 5 we show AIRs, BER and used constellations for $R = 4/5$ and $M = 64$. The recommended IBO from [11] is IBO $= 3.25$ dB. We use this IBO as the initial value for training of the power back-off.

	APSK no IBO opt.	APSK with IBO opt.	NUC	Trained APSK
IBO	3.25 dB	4.87 dB	5.054 dB	5.10 dB
OBO	4.09 dB	4.32 dB	4.26 dB	4.39 dB

TABLE II: IBO and OBO for $M = 64$ and $R = 4/5$.

	APSK no IBO opt.	APSK with IBO opt.	NUC	Trained APSK
IBO	4.25 dB	5.2 dB	5.09 dB	4.99 dB
OBO	4.96 dB	5.05 dB	4.92 dB	4.79 dB

TABLE III: IBO and OBO for $M = 256$ and $R = 20/30$.

For all training setups, the learned IBO and resulting OBO are summarized in Table II for $M = 64$.

The information rate is highest for the trained APSK of Fig. 5c followed by the two configurations with the APSK from DVB-S2X (Fig. 5a). The NUC of Fig. 5b yields the worst performance for this configuration. In BER performance, the optimized APSK yields the best performance as well. The BER does not outperform the recommended quasi error-free performance (gray line) from DVB-S2X, which was simulated on an ideal limiter channel. In contrast, we have used the model (2), (3) and included the IMUX and OMUX filters into our simulations, which results in a more realistic and hence, more challenging setup, particularly for high code rates.

MODCOD 20/30 Modulation Order 256: For $M = 256$ and code rate $R = 20/30$, DVB-S2X recommends the constellation displayed in Fig. 6a. This constellation is an irregular APSK, where the innermost points are not perfect circles and may have been optimized similar to NUC constellations, as the constellation shows a quadrant symmetry. To optimize an APSK constellation with arbitrary phase shifts, we initialized with a different constellation. For $M = 256$, a regular APSK is for $M = 256$ defined under MODCOD 116/180 in DVB-S2X. This 256 APSK has 8 rings and 32 points per ring, where we optimize radii of each ring and phases of each point. The result is displayed in Fig. 6c. The performance of the trained APSK is inferior to NUC and the constellation from DVB-S2X, in contrast to the prior analysis for $M = 64$ and $R = 4/5$. This, and the fact that Fig. 6a is not a regular APSK indicates, that regular APSK constellations may not be ideal for $R = 20/30$ and $M = 256$. In contrast, the autoencoder with NUC optimization (Fig. 6b) yields a constellation with competitive performance to the DVB-S2X constellation (Fig. 6a). The best performance in BER is, however, found for the DVB-S2X constellations with optimized IBO. For $M = 256$, the optimized IBO and resulting OBO are summarized in Table III.

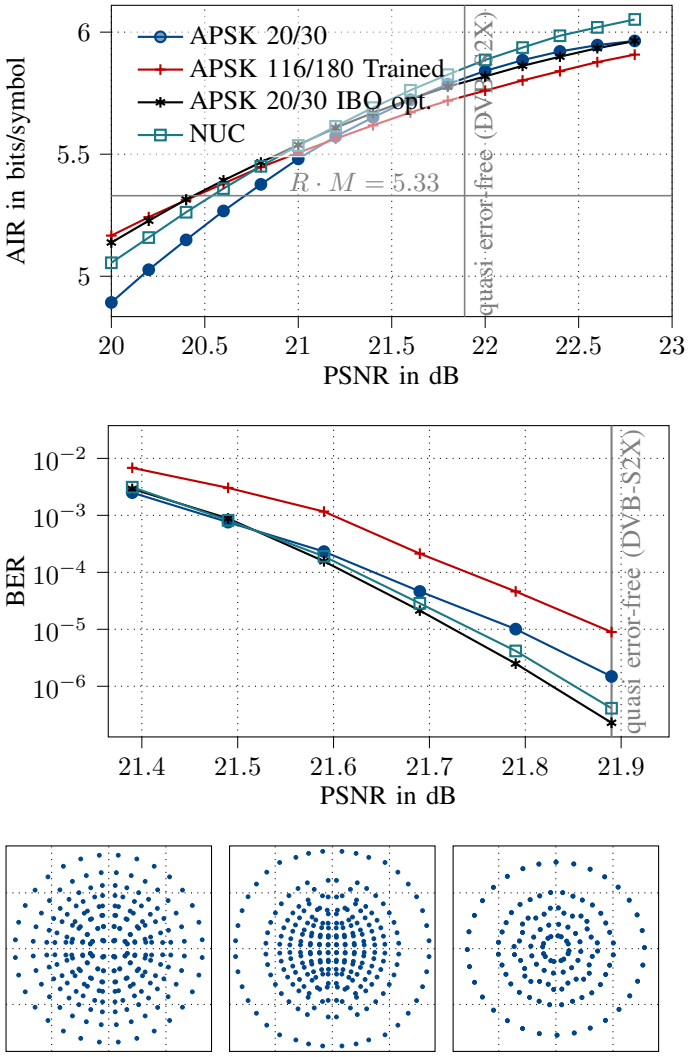

(a) APSK MODCOD 20/30 DVB-S2X.

(b) NUC.

(c) APSK trained based on MODCOD 116/180.

Fig. 6: AIR, BER and trained constellations for $R = 20/30$ and $M = 256$.

IV. Conclusion

This work proposed a concept to jointly train constellations, power back-off and predistortion for efficient transmission over transparent satellite transponders. By means of communication autoencoders, the transmitter is adapted to the power amplifier to maximize the transmit power while minimizing the nonlinear distortions caused by amplifier saturation. We have shown how different constellation shaping schemes improve the performance compared to the recommended APSK constellations from the satellite broadcasting standard DVB-S2X. The goal of this work was to show how neural networks can contribute to maximize the throughput of transmissions over satellite payloads.

References

[1] H. Shahid, C. Amatetti, R. Campana, S. Tong, D. Panaitopol, A. V. Coralli, A. Mohamed, C. Zhang, E. Khalifa, E. Medeiros, E. Recayte, F. Ghasemifard, J. Lianghai, J. Bucheli, K. A. Swamy, M. Caus, M. Gurelli, M. A. Vazquez, M. Shaat, N. Borios, P.-E. Eriksson, S. Euler, Z. Li, and X. Fu, "Emerging Advancements in 6G NTN Radio Access Technologies: An Overview," Apr. 2024.

[2] E. Casini, R. D. Gaudenzi, and A. Ginesi, "DVB-S2 modem algorithms design and performance over typical satellite channels," *International Journal of Satellite Communications and Networking*, vol. 22, no. 3, pp. 281–318, 2004.

[3] A. Bazzi and M. Chafii, "On Integrated Sensing and Communication Waveforms With Tunable PAPR," *IEEE Transactions on Wireless Communications*, vol. 22, no. 11, pp. 7345–7360, Nov. 2023.

[4] "Second generation framing structure, channel coding and modulation systems for Broadcasting, Interactive Services, News Gathering and other broadband satellite applications; Part 2: DVB-S2 Extensions (DVB-S2X)," http://www.etsi.org.

[5] D. Kopyto and G. Bauch, "Recurrent Neural Network Data Predistortion for Transparent Satellite Channels," in *GLOBECOM 2024 - 2024 IEEE Global Communications Conference*, Cape Town, Dec. 2024.

[6] R. De Gaudenzi, A. Guillen i Fabregas, and A. Martinez, "Performance analysis of turbo-coded APSK modulations over nonlinear satellite channels," *IEEE Transactions on Wireless Communications*, vol. 5, no. 9, pp. 2396–2407, Sep. 2006.

[7] A. Modenini, A. Ugolini, and G. Colavolpe, "A Fast Method for optimizing the Amplifier Output Back-off by Means of the Total Degradation," in *2019 8th International Workshop on Tracking, Telemetry and Command Systems for Space Applications (TTC)*, Sep. 2019, pp. 1–6.

[8] T. O'Shea and J. Hoydis, "An Introduction to Deep Learning for the Physical Layer," *IEEE Transactions on Cognitive Communications and Networking*, vol. 3, no. 4, pp. 563–575, Dec. 2017.

[9] S. Cammerer, F. A. Aoudia, S. Dörner, M. Stark, J. Hoydis, and S. ten Brink, "Trainable Communication Systems: Concepts and Prototype," *IEEE Transactions on Communications*, vol. 68, no. 9, pp. 5489–5503, Sep. 2020.

[10] D. Kopyto and G. Bauch, "Neural Constellation Shaping and Back-Off Training for Memoryless Power Amplifiers," in *2024 IEEE Wireless Communications and Networking Conference (WCNC)*, Apr. 2024, pp. 1–6.

[11] "Implementation guidelines for the second generation system for Broadcasting, Interactive Services, News Gathering and other broadband satellite applications; Part 2: S2 Extensions (DVB-S2X)," https://dvb.org/?standard=dvb-s2x-implementation-guidelines.

[12] A. Saleh, "Frequency-Independent and Frequency-Dependent Nonlinear Models of TWT Amplifiers," *IEEE Transactions on Communications*, vol. 29, no. 11, pp. 1715–1720, Nov. 1981.

[13] M. Schetzen, *The Volterra and Wiener Theories of Nonlinear Systems*. USA: Krieger Publishing Co., Inc., Mar. 2006.

[14] M. H. Moghaddam, S. R. Aghdam, N. Mazzali, and T. Eriksson, "Statistical Modeling and Analysis of Power Amplifier Nonlinearities in Communication Systems," *IEEE Transactions on Communications*, vol. 70, no. 2, pp. 822–835, Feb. 2022.

[15] M. Stark, F. Ait Aoudia, and J. Hoydis, "Joint Learning of Geometric and Probabilistic Constellation Shaping," in *2019 IEEE Globecom Workshops (GC Wkshps)*, Dec. 2019, pp. 1–6.

[16] N. S. Loghin, J. Zöllner, B. Mouhouche, D. Ansorregui, J. Kim, and S.-I. Park, "Non-Uniform Constellations for ATSC 3.0," *IEEE Transactions on Broadcasting*, vol. 62, no. 1, pp. 197–203, Mar. 2016.

[17] D. Yoda and H. Ochiai, "Decision Region Optimization and Metric-Based Compensation of Memoryless Nonlinearity for APSK Systems," *IEEE Transactions on Broadcasting*, vol. 64, no. 2, pp. 281–292, Jun. 2018.

[18] J. Hoydis, S. Cammerer, F. A. Aoudia, A. Vem, N. Binder, G. Marcus, and A. Keller, "Sionna: An Open-Source Library for Next-Generation Physical Layer Research," Mar. 2022.